4,4′-Bis(2-picolinimino)-2,2′-bibenzimidazoles: A New Class of Dinucleating Ligands Which Allow for a Tuning of the Metal–Metal Distance. Structures and Properties of a Dicopper(II) Complex and of Two Oxygenation Products of a Dicopper(I) Complex: A Tentative Coordination Chemical Modeling of Hemocyanin

Edgar Müller,*,† Gérald Bernardinelli,‡ and Jan Reedijk†

Leiden Institute of Chemistry, Gorlaeus Laboratories, Leiden University, P.O. Box 9502, 2300 RA Leiden, The Netherlands, and Laboratoire de Cristallographie, Université de Genève, 24 Quai Ernest Ansermet, 1211 Genève, Switzerland

Received March 8, 1995[⊗]

The title compounds (**L**), derived from 1,1′-disubstituted 4,4′-diamino-2,2′-bibenzimidazoles and 2-pyridinecarboxaldehyde, were developed as models for type 3 sites of the copper proteins *hemocyanin* and *tyrosinase*. These hollow, ditopic ligands can hold two metal ions face to face at distances of 3.15 Å or larger. The metal–metal distance can be restricted (tuned) to a given value via a corresponding polymethylene bridge in the ligand's backbone. The complex $[Cu^{II}_2(\mathbf{L})(dmf)_3(H_2O)_2](F_3CSO_3)_4$ of the unrestricted ligand 1,1′,5,5′,6,6′-hexamethyl-4,4′-bis(2-picolinimino)-2,2′-bibenzimidazole (**L**) (space group *P*-1, $a = 14.811(21)$ Å, $b = 15.358(26)$ Å, $c = 16.209(9)$ Å, $\alpha = 95.57(9)°$, $\beta = 107.56(9)°$, $\gamma = 110.35(13)°$, $Z = 2$) presents an open conformation with discrete (4 + 2) copper coordination environments, where two dimethylformamide (dmf) molecules occupy the fourth positions of the equatorial CuN_3O squares ($\langle Cu-N\rangle = 2.02$ Å, $\langle Cu-O\rangle = 1.95$ Å). Two water molecules, a dmf and one of the triflate anions, are coordinated to the four axial positions (Cu–O of 2.28–2.74 Å). The two halves of the ligand are rotated out of the cis-coplanar conformation by 115.7°, resulting in a relatively long Cu···Cu distance of 6.16 Å. In acetonitrile, the complex shows two irreversible Cu(II)/Cu(I) redox potentials at 0.60 and 0.30 V (NHE). Two oxygenation products of the dicopper(I) complex of the restricted ligand 1,1′-trimethylene-5,5′,6,6′-tetramethyl-4,4′-bis(2-picolinimino)-2,2′-bibenzimidazole (**L3**), which best approaches the geometry of a type 3 site, were isolated in the crystalline state. The first one, $[Cu^{II}_4(H_2(\mathbf{L3})O_2^{2-})_2](ClO_4)_4$ (orthorhombic: *Ccca*, $a = 16.171(3)$ Å, $b = 19.760(4)$ Å, $c = 22.168(5)$ Å, $Z = 4$), is a tetranuclear copper(II) cluster, best described as a symmetric Cu_4O_4 eight membered ring (Cu···Cu distances of 3.05, 3.50, and 6.30 Å), attached to two **L3** molecules, with the four oxy anions covalently linked to the azomethine carbons (forming the **L3** derivative $H_2(\mathbf{L3})O_2^{2-}$). The second oxygenation product, $[Cu^{I}_2(\mathbf{L3}')_2](ClO_4)_2$ (monoclinic: *C*2/*c*, $a = 23.500(3)$ Å, $b = 12.569(5)$ Å, $c = 19.926(8)$ Å, $\beta = 106.71(2)°$, $Z = 4$), is a dinuclear copper(I) complex of **L3′**, a degradation product of **L3**, carrying a free amino group on one side. The copper(II) ions are in a bis(diimine) type, distorted tetrahedral environment (dihedral angle 79.1°), with a Cu···Cu distance of 4.59 Å. About 25% of the ligand **L3′** appears to be oxidized at the free amino group to the corresponding quinonimine, as deduced from the X-ray structure determination.

Introduction

The active sites of *hemocyanin*[1] and *tyrosinase*[2] both consist of a similar structural unit containing two antiferromagnetically coupled copper ions which are held at a distance of 3.55 Å by the protein environment. The ions are facing each other with a void between them (Chart 1). The dicopper(I) (=deoxy) species reacts reversibly with dioxygen ($^3O_2$); the resulting bis(copper(II)–μ-peroxo) (=oxy) species contains a coordinated O_2^{2-} ion in the void.[1a] The same species may be obtained from the dicopper(II) (=met) derivative and hydrogen peroxide (H_2O_2). Analogous type 3 copper sites are accepted or known to occur in *laccase* and *ascorbate oxidase*; the structure of the latter has recently been published.[3] The Cu(II)/Cu(I) potentials

Chart 1. Active Site of Hemocyanin

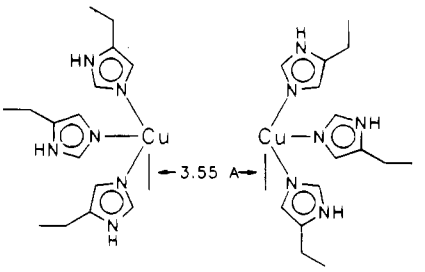

† Leiden University.

‡ Université de Genève.

⊗ Abstract published in *Advance ACS Abstracts,* October 15, 1995.

(1) (a) Magnus, K. A.; Hazes, B.; Ton-That, H.; Bonaventura, C.; Bonaventura, J.; Hol, W. G. J. *Biochem. J.* **1993**, 55–63, and references cited therein. (b) Gaykema, W. P. J.; Volbeda, A.; Hol, W. G. J. *J. Mol. Biol.* **1985**, *187*, 255–275; **1989**, *209*, 249–279. (c) *Copper Coordination Chemistry: Biochemical and Inorganic Perspectives*; Karlin, K. D., Zubieta, J., Eds.; Adenine: New York, 1983. (d) Spiro, T. G.; Woolery, G. L.; Brown, J. M.; Powers, L.; Winkler, M. E.; Solomon, E. I. In *Copper Coordination Chemistry: Biochemical and Inorganic Perspectives*; Karlin, K. D., Zubieta, J., Eds.; Adenine: New York, 1983; pp 23–41. (e) Magnus, K. A.; Ton-That, H.; Carpenter, J. E. *Chem. Rev.* **1994**, *94*, 727–735.

(2) (a) Solomon, E. I. *Pure Appl. Chem.* **1983**, *55*, 1069–1088. (b) Wilcox, D. E.; Porras, A. G.; Hwang, Y. T.; Lerch, K.; Winkler, M. E.; Solomon, E. I. *J. Am. Chem. Soc.* **1985**, *107*, 4015–4027.

(3) (a) Messerschmidt, A.; Rossi, A.; Ladenstein, R.; Huber, R.; Bolognesi, M.; Gatti, G.; Marchesini, A.; Petruzelli, R., Finazzo-Agró, A. *J. Mol. Biol.* **1989**, *206*, 513. (b) Messerschmidt, A.; Ladenstein, R.; Huber, R.; Bolognesi, M.; Avigliano, L.; Petruzelli, R.; Rossi, A.; Finazzi-Agró, A. Refined structure of ascorbate oxidase at 1.9 Å resolution. *J. Mol. Biol.* **1992**, *224*, 179–205.

0020-1669/95/1334-5979$09.00/0

of such sites lie in the region of 360 mV vs NHE.[4] When the copper site is not as protected (buried) as in hemocyanin,[5] the addition product of the type 3 site with dioxygen may undergo autoxidation, or hydroxylate/oxidize aromatic nuclei and other suitable substrates (*tyrosinase* activity).[6] The electrophilic nature of these reactions has recently been put in evidence.[7]

Much work has been undertaken during the past decade with the aim of understanding and modeling the type 3 dinuclear copper site,[8] especially by the groups of Karlin and of Kitajima; the subject has also been reviewed by Martell, Sorrell and Fenton, as well as by Magnus and Kitajima.[9] Two structures of an "end-on" and a "side-on" dicopper–μ-peroxo complex have been published recently,[10] as has the structure of *Limulus polyphemus oxyhemocyanin*.[1a] From these, as from the structure of the *Panuliris interruptus deoxyhemocyanin*,[1b] it follows that dioxygen binding requires a Cu–Cu distance on the order of 3.5 Å.

A feature widely neglected in most of the published hemocyanin models is, however, the protein's predisposed and highly copper specific site geometry, consisting of three conveniently oriented histidyl residues in an otherwise rigid, hydrophobic, and hardly accessible environment.[5] Overlooking or neglecting the assembling and protecting role of the ligand system results in a low thermodynamic stability of the model dioxygen adducts and in their ease of undergoing unwanted secondary reactions. In fact, most of the described copper–dioxygen complexes could only be prepared, studied, and crystallized at low temperatures, which is in striking contrast to the reversible room temperature chemistry of natural hemocyanin. The enthalpies of formation of model dicopper–dioxygen adducts are reported to be favorable by about 60 kJ/mol and similar to the values found in natural hemocyanins. The poor room temperature stability of the discussed model systems has therefore to be traced back to the high entropy of formation involved in the assembly of the dicopper–dioxygen aggregates[11] from too many individual or flexible components, as well as to the lack of a convenient site protection.

Our attempt to model the type 3 site was aimed at a better imitation of the protein's function in defining and protecting the site; we therefore looked for a ligand system able to create a hollow, ditopic receptor for two copper ions, disposed at the right distance in an otherwise rigid environment. 4,4′-Diamino-2,2′-bibenzimidazole was chosen as the ligand's backbone, as it spans a distance of 8 Å between the two amino groups and allows them to be conformationally fixed or restricted, if needed, through the introduction of an additional polymethylene bridge between the benzimidazole nitrogen atoms opposite to the coordination site. Precursors for this type of ligand can be found in the work of Schugar[12] and Thummel.[13] The model ligand would then be completed by two or four pendant coordinating substituents, attached to the 4,4′-amino groups.

On the basis of previous work,[14] a ligand with four substituted pyridyl side chains, as shown in Chart 2, was tagged as uniting

(4) Kida, S.; Okawa, H.; Nishida, Y. In *Copper Coordination Chemistry: Biochemical and Inorganic Perspectives*; Karlin, K. D., Zubieta, J., Eds.; Adenine: New York, 1983; pp 425–444.

(5) (a) Vollbeda, A.; Hol, W. G. J. The 3.2 Å resolution X-ray structure of *Panuliris interruptus* haemocyanin. Ph.D. Thesis, Groningen State University, Groningen, Netherlands, 1988. (b) Hazes, B.; Magnus, K. A.; Bonaventura, C.; Bonaventura, J.; Dauter, Z.; Kalk, K. H.; Hol, W. G. J. Crystal structure of deoxygenated *Limulus polyphemus* subunit II haemocyanin at 2.18 Å resolution: Clues for a mechanism for allosteric regulation. *Protein Sci.* **1993**, *2*, 597–619.

(6) Karlin, K. D.; Hayes, J. C.; Gultneh, Y.; Cruse, R. W.; McKown, J. W.; Hutchinson, J. P.; Zubieta, J. *J. Am. Chem. Soc.* **1984**, *106*, 2121–2128. Cruse, R. W.; Kaderli, S.; Karlin, K. D.; Zuberbühler, A. D. *J. Am. Chem. Soc.* **1988**, *110*, 6882–6883. Patch, M. G.; McKee, V.; Reed, C. A. *Inorg. Chem.* **1987**, *26*, 776–778. Davies, G.; El-Sayed, M. A.; Henary, M. *Inorg. Chem.* **1987**, *26*, 3266–3273. El-Sayed, M. A.; Abu-Raqabah, A. A.; Davies, G.; El-Toukhy, A. *Inorg. Chem.* **1989**, *28*, 1909–1914. Cabral, M. F.; Cabral, J.; Trocha-Grimshaw, J.; McKillop, K. P.; Nelson, S. M.; Nelson J. *J. Chem. Soc., Dalton Trans.* **1989**, 1351–1359. Réglier, M.; Amadeï, E.; Tadayoni, R.; Waegell, B. *J. Chem. Soc., Chem. Commun.* **1989**, 447–450. Sorrell, T. N.; Vankai, V. A. *Inorg. Chem.* **1990**, *29*, 1687–1692. Gelling, O. J.; Meetsma, A.; Feringa, B. L. *Inorg. Chem.* **1990**, *29*, 2816–2822.

(7) (a) Nasir, M. S.; Cohen, B. I.; Karlin, K. D. *J. Am. Chem. Soc.* **1992**, *114*, 2482–2494. (b) Sheldon, R. A.; Kochi, J. K. *Metal-Catalyzed Oxydations of Organic Compounds*; Academic Press: New York, **1981**. (c) Kurata, T.; Watanabe, Y.; Katoh, M.; Sawaki, Y. *J. Am. Chem. Soc.* **1988**, 110, 7472–7478.

(8) (a) Karlin, K. D.; Fox, S.; Nanthakumar, A.; Murthy, N. N.; Wei, N.; Obias, H. V.; Martens, C. F. *Pure Appl. Chem.* **1995**, *67*, 289–296. Tyeklár, Z.; Jacobson, R. R.; Wei, N.; Murthy, N. N.; Zubieta, J.; Karlin, K. D. *J. Am. Chem. Soc.* **1993**, *115*, 2677–2689. Sanyal, I.; Mahroof-Tahir, M.; Nasir, M. S.; Ghosh, P.; Cohen, B. I.; Gultneh, Y.; Cruse, R. W.; Farooq, A.; Karlin, K. D.; Liu, S.; Zubieta, J. *Inorg. Chem.* **1992**, *31*, 4322–4332. Karlin, K. D.; Tyeklár, Z.; Farooq, A.; Haka, M. S.; Ghosh, P.; Cruse, R. W.; Gultneh, Y.; Hayes, J. C.; Toscano, P. J.; Zubieta, J. *Inorg. Chem.* **1992**, *31*, 1436–1451. Mahroof-Tahir, M.; Murthy, N. N.; Karlin, K. D.; Blackburn, N. J.; Shaikh, S. N.; Zubieta, J.; *Inorg. Chem.* **1992**, *31*, 3001–3003. Mahroof-Tahir, M.; Karlin, K. D. *J. Am. Chem. Soc.* **1992**, *114*, 7599–7601. Baldwin, M. J.; Ross, P. K.; Pate, J. E.; Tyeklár, Z.; Karlin, K. D.; Solomon, E. I. *J. Am. Chem. Soc.* **1991**, *113*, 8671–8679. Karlin, K. D.; Wei, N.; Jung, B.; Kaderli, S.; Zuberbühler, A. D. *J. Am. Chem. Soc.* **1991**, *113*, 5868–5870. Paul, P. P.; Tyeklár, Z.; Jacobson, R. R.; Karlin, K. D. *J. Am. Chem. Soc.* **1991**, *113*, 5322–5332. Sanyal, I.; Strange, R. W.; Blackburn, N. J.; Karlin, K. D. *J. Am. Chem. Soc.* **1991**, *113*, 4693–4694. Nasir, M. S.; Karlin, K. D.; McGowty, D.; Zubieta, J. *J. Am. Chem. Soc.* **1991**, *113*, 698–700. Karlin, K. D.; Gan, Q.-F.; Farooq, A.; Liu, S. Zubieta, J. *Inorg. Chem.* **1990**, *29*, 5249–5251. Karlin, K. D.; Cruse, R. W.; Gultneh, Y.; Farooq, A.; Hayes, J. C.; Zubieta, J. *J. Am. Chem. Soc.* **1987**, *109*, 2668–2679. Blackburn, N. J.; Karlin, K. D.; Concannon, M.; Hayes, J. C.; Gultneh, Y.; Zubieta, J. *J. Chem. Soc., Chem. Commun.* **1984**, 939–984. Karlin, K. D.; Gultneh, Y.; Hayes, J. C.; Zubieta, J.; *Inorg. Chem.* **1984**, *23*, 519–521. (b) Kitajima, N.; Katayama, T.; Fujisawa, K.; Iwata, Y.; Moro-oka, Y.; *J. Am. Chem. Soc.* **1993**, *115*, 7872–7875. Baldwin, M. J.; Root, D. E.; Pate, J. E.; Fujisawa, K.; Kitajima, N.; Solomon, E. I. *J. Am. Chem. Soc.* **1992**, *114*, 10421–10431. Kitajima, N.; Fujisawa, K.; Fujimoto, C.; Moro-oka, Y.; Hashimoto, S.; Kitagawa, T.; Toriumi, K.; Tatsumi, K.; Nakamura, A. *J. Am. Chem. Soc.* **1992**, *114*, 1277–1291. Kitajima, N.; Koda, T.; Hashimoto, S.; Kitagawa, T.; Moro-oka, Y. *J. Am. Chem. Soc.* **1991**, *113*, 5664–5671. Kitajima, N.; Fujisawa, K.; Moro-oka, Y. *Inorg. Chem.* **1990**, *29*, 357–358. Kitajima, N.; Koda, T.; Iwata, Y.; Moro-oka, Y. *J. Am. Chem. Soc.* **1990**, *112*, 8833–8839. (c) McKee, V.; Zvagulis, M.; Dagdigian, J. V.; Patch, M. G.; Reed, C. A. *J. Am. Chem. Soc.* **1984**, *106*, 4765–4772. (d) Rockcliffe, D. A.; Martell, A. E. *Inorg. Chem.* **1993**, *32*, 3143–3152. (e) Sorrell, T. N.; Borovik, A. S. *J. Chem. Soc., Chem. Commun.* **1984**, 1489. Sorrell, T. N.; Jameson, D. L.; O'Connor, C. J. *Inorg. Chem.* **1984**, *23*, 190–195. (f) Berends, H. P.; Stephan, D. W. *Inorg. Chem.* **1987**, *26*, 749–754. (g) Simmons, M. G.; Wilson, L. J. *J. Chem. Soc., Chem. Commun.* **1978**, 634. Goodwin, J. A.; Bodager, G. A.; Wilson, L. J.; Stanbury, D. M.; Scheidt, W. R. *Inorg. Chem.* **1989**, *28*, 35–42. (h) Van Rijn, J.; Reedijk, J.; Dartmann, M.; Krebs, B. *J. Chem. Soc., Dalton Trans.* **1987**, 2579. Birker, P. J. M. W. L.; Reedijk, J. In *Copper Coordination Chemistry: Biochemical and Inorganic Perspectives*; Karlin, K. D., Zubieta, J., Eds.; Adenine: New York, 1983; pp 409–424. (i) Piguet, C.; Bocquet, B.; Müller, E.; Williams, A. F.; *Helv. Chim. Acta* **1989**, *72*, 323–337.

(9) (a) Martell, A. E. Oxydation of Organic Stubstrates with Dioxygen Complexes as Intermediates. *Pure Appl. Chem.* **1983**, *55*, 125–135. (b) Sorrell, T. N. Tetrahedron Report 246. *Tetrahedron* **1989**, *45*, 3–68. (c) Vigato, P. A.; Tamburini, S.; Fenton, D. E. The Activation of Small Molecules by Dinuclear Complexes of Copper and Other Metals. *Coord. Chem. Rev.* **1990**, *106*, 25–170. (d) Fenton, D. E. From Crowns to Clefts: Synthetic Analogs for Type 3 Copper Centres. in *Perspectives in Coordination Chemistry*; Williams, A. F., Floriani, C., Merbach, A. E., Eds.; VHCA and VCH: Basel, Switzerland, and Weinheim, Germany, 1992; pp 203–218. (e) Magnus, K. A.; Ton-That, H.; Carpenter, J. E. *Chem. Rev.* **1994**, *94*, 727–735. (f) Kitajima, N.; Moro-oka, Y. *Chem. Rev.* **1994**, *94*, 737–757.

(10) (a) Jacobson, R. R.; Tyeklar, Z.; Farooq, A.; Karlin, K. D.; Liu, S.; Zubieta, J. *J. Am. Chem. Soc.* **1988**, *110*, 3690–3692. Tyeklar, Z.; Paul, P. P.; Jacobson, R. R.; Farooq, A.; Karlin, K. D.; Zubieta, J. *J. Am. Chem. Soc.* **1989**, *111*, 388–389, and references cited herein. (b) Kitajima, N.; Fujisawa, K.; Moro-oka, Y. *J. Am. Chem. Soc.* **1989**, *111*, 8975–8976. Kitajima, N.; Moro-oka, Y. Abstracts of ICBIC-4, L008. *J. Inorg. Biochem.* **1989**, *36*, 310. Kitajima, N.; Koda, T.; Hashimoto, S.; Kitagawa, T.; Moro-oka, Y. *J. Chem. Soc., Chem. Commun.* **1988**, 151.

Chart 2. Target Model Ligand System

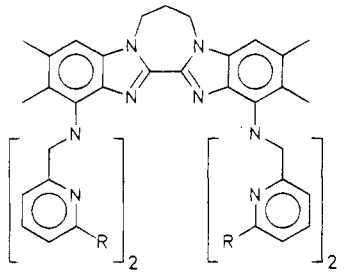

Chart 3. Simplified Schiff Base Ligands (with Their Acronyms)

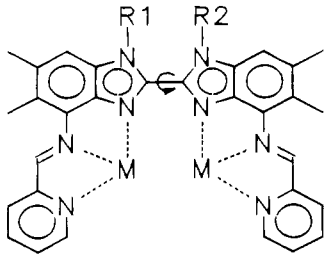

R1	R2	
$-CH_3$	$-CH_3$	L
$-(CH_2)_2-$		L2
$-(CH_2)_3-$		L3
$-(CH_2)_4-$		L4

the required conditions: a metal−metal distance in the range of 3.5 Å, "buried" metal ions in the center of the complex, and a site protection by the pyridyl's terminal bulky or long chained R-groups. We expected such a ligand to facilitate the access to a room temperature stable dicopper−μ-peroxo species. At a previous stage and due to synthetic difficulties, complexes of the easier obtainable Schiff base ligands with only two pyridyl side chains, shown in Chart 3, were studied. They already possess some unique features, inasmuch as their two N_3-subunits can be rotated against each other, and in this way, the metal−metal distance can be varied (tuned). In the following, we describe the synthetic route to this new class of ligands and present the first results of their copper−dioxygen chemistry.

Experimental Section

Physical Measurements. IR spectra were recorded on a Perkin Elmer 580; UV/vis spectra on a Perkin Elmer 330; ^{1}H-NMR spectra, on a Bruker FX 200 instrument. Cyclic voltammograms were taken at a glassy carbon electrode under N_2, using a BAS CV-1B potentiostat, coupled to a BAS C-1A cell stand and a BAS *X*−*Y* recorder. Tetrabutylammonium perchlorate (TBAP) 0.1 M served as the supporting electrolyte in acetonitrile. The reference potential was taken with an Ag^+/Ag electrode and standardized against the known potentials of the $[Ru(bpy)_3]^{2+}$ cation under the same conditions. The voltammograms were analyzed according to established procedures.[15] Elemental analyses were carried out by University College Dublin; mass spectra were obtained on a Finnigan MAT 900 instrument in EI mode with a direct insertion probe. Q-band EPR spectra were measured on a Varian E-9, using a Bruker ER 061 SR microwave bridge.

Analyses. All of the simple 2,2′-bibenzimidazole derivatives turned out to have rather low solubilities in the common solvents and showed high melting points (>250 °C). ^{13}C NMR spectra could not be obtained. In order to allow for a proper identification of the compounds, ^{1}H NMR, IR, MS, and elemental analyses data are given. In the final oxygenation experiment, X-ray structure determination was used as an analytic tool.[29]

X-ray Structure Determinations. Details of the X-ray determinations are given in Table 1; results, in Tables 2−7. All data sets were measured on an Enraf-Nonius CAD-4 instrument, using graphite monochromatized Mo Kα radiation (Λ = 0.710 69 Å). The structures were solved and refined using the MULTAN-78,[16] MULTAN-87,[17] SHELX-76 and SHELXS-86,[18] XTAL 3.0,[19] REDDIF83,[20] and KLKWAD88[21] programs. Scattering factors and related crystallographic information were taken from the "International Tables".[22] Drawings were made with ORTEP.[23]

Starting Materials. Chemicals and solvents were purchased from Janssen Chimica (Beerse, Belgium). 4,5-Dimethyl-1,2-phenylenediamine was purchased from Aldrich. Sodium hydride suspension in mineral oil and tetramethylurea (tmu) were purchased from Fluka (Buchs, Switzerland). Tetramethylurea was distilled under reduced pressure from sodium hydride prior to use.

Crystalline $[Cu(MeCN)_4]ClO_4$ was prepared by reduction of commercial $[Cu(H_2O)_6](ClO_4)_2$ in acetonitrile (MeCN) with copper powder at 40 °C, filtering and cooling the resulting colorless solution in ice. *Caution*: Perchlorate salts of metal complexes with organic ligands are potentially explosive and should be handled with care![24]

An overview of the ligand syntheses is given in Scheme 1. Entry into the 2,2′-bibenzimidazole system through condensation of an *o*-phenylenediamine with an oxalic acid derivative[25] resulted in a very impure product. A better procedure[26] uses trichloroacetimidate or trichloroacetonitrile instead of oxalic derivatives. In the following, we give a simple one-step procedure, starting from trichloroacetic acid and *o*-phenylenediamines, which results in a quantitative yield of isomerically pure 2,2′-bibenzimidazoles.

5,6,5′,6′-Tetramethyl-2,2′-bibenzimidazole: In an open, 250-mL round-bottom flask equipped with magnetic stirring, 13.6 g (0.1 mol) of 4,5-dimethyl-1,2-phenylenediamine was heated with 16.3 g (0.1 mol) of trichloroacetic acid in 50 mL of 85% orthophosphoric acid during 2 h, progressively to an end temperature of 180 °C. At 120 °C, the reaction mixture was strongly frothing, and further heating had to occur with care. The condensation proceeded with the evolution of water and hydrogen chloride vapors, and a homogeneous, green-brown melt was finally obtained. This melt was hydrolyzed with 200 mL of water, and the off-white precipitate of the dihydrogen phosphate was filtered and neutralized with excess dilute ammonia. The precipitated free base

(11) (a) Zuberbühler, A. D. Abstracts of ICBIC-4, L010. *J. Inorg. Biochem.* **1989**, *36*, 311. Cruse, R. W.; Kaderli, S.; Meyer, C. J.; Zuberbühler, A. D.; Karlin, K. D. *J. Am. Chem. Soc.* **1988**, *110*, 5020−5024. (b) Karlin, K. D.; Ghosh, P.; Cruse, R. W.; Farooq, A.; Gultneh, Y.; Jacobson, R. R.; Black-burn, N. J.; Strange, R. W.; Zubieta, J. *J. Am. Chem. Soc.* **1988**, *110*, 6769−6780.
(12) Knapp, S.; Keenan, T. P.; Zhang, X.; Fikar, R.; Potenza, J. A.; Schugar, H. J. *J. Am. Chem. Soc.* **1987**, *109*, 1882−1883.
(13) Goulle, V.; Thummel, R. P. *Inorg. Chem.* **1990**, *29*, 1767−1772.
(14) Cf. refs 8h,i.
(15) Bard, A. J.; Faulkner, L. R. *Electrochemical Methods, Fundamentals and Applications*; Wiley: New York, 1980; Chapter 6.
(16) Main, P.; Lessinger, L.; Woolfson, M. M.; Germain, G.; Declercq, J.-P. *MULTAN, A System of Computer Programs for the Automatic Solution of Crystal Structures from X-ray Diffraction Data*; Universities of York, York, England, and Louvain, Louvain-La-Neuve, Belgium, 1978.
(17) Main, P.; Fiske, S. J.; Hull, S. E.; Lessinger, L.; Germain, D.; Declercq, J. P.; Woolfson, M. M. MULTAN 87; Universities of York, York, England, and Louvain, Louvain-La-Neuve, Belgium, 1987.
(18) Sheldrick, G. Institut für Anorganische Chemie der Universität, Tammanstrasse 4, D-3400 Göttingen, Germany.
(19) Hall, S. R., Stewart, J. M., Eds. XTAL 3.0. *User's Manual*; Universities of Western Australia and Maryland: Nedlands, Australia, and College Park, MD, 1989.
(20) De Graaff, R. A. G.; Verschoor, G. C.; Gorter, S. Program REDDIF83, Leiden University, 1983.
(21) Rutten-Keulemans, E. Program KLKWAD88, Leiden University, 1988.
(22) *International Tables for X-ray Crystallography*; Kynoch, Birmingham, England, 1974.
(23) Johnson, C. K.*ORTEP II*, Report ORNL-5138. Oak Ridge National Laboratory: Oak Ridge, TN, 1976.
(24) Wolsey, W. C. *J. Chem. Educ.* **1973**, *50*, A335; *Chem. Eng. News* **1963**, *41*, 47. Raymond, K. N. *Chem. Eng. News* **1983**, *61*, 4.
(25) (a) Constable, E. C.; Steel, P. J. *Coord. Chem. Rev.* **1989**, *93*, 205−223, and references cited therein. (b) Hünig, S.; Scheutzow, D.; Schlaf, H.; Quast, H. *Liebigs Ann. Chem.* **1972**, *765*, 110−125.
(26) Holan, G.; Samuel, E. L.; Ennis, B. C.; Hinde, R. W. *J. Chem. Soc. C* **1967**, 20−39.

Table 1. Summary of Crystal and X-ray Structure Determination Data

cation	$[Cu^{II}_2(\mathbf{L})(dmf)_3(H_2O)_2]^{4+}$	$[Cu^{II}_4(H_2(\mathbf{L3})O_2^{2-})_2]^{4+}$	$[Cu^{I}_2(\mathbf{L3'})_2]^{2+}$
formula	$Cu_2C_{45}H_{55}F_{12}N_{11}O_{17}S_4$	$Cu_4C_{66}H_{64}Cl_4N_{16}O_{20}$	$Cu_2C_{54}H_{52}Cl_2N_{14}O_{8.25}$
MW	1505.31	1797.32	1227.09
cryst syst	triclinic	orthorhombic	monoclinic
space group	*P*-1	*Ccca*	*C*2/*c*
a (Å)	14.811(21)	16.171(3)	23.500(3)
b (Å)	15.358(26)	19.760(4)	12.569(5)
c (Å)	16.209(9)	22.168(5)	19.926(8)
α (deg)	95.57(9)	90.0	90.0
β (deg)	107.56(9)	90.0	106.71(2)
γ (deg)	110.35(13)	90.0	90.0
V (Å^3)	3210.7	7083.5	5637.1
Z	2	4	4
data collecn	ω (0−22°)	$\omega/2\theta$ (0−22°)	ω (0−22°)
unique reflecn	11279	2167	2737
obsd reflecn	4086 (>2σ)	912 (>4σ)	504 (>2σ)
params	820	250	149
R (unit weights)	0.057	0.106	0.069

Table 2. Non-Hydrogen Positional, Isotropic Displacement, and Occupation Parameters for $[Cu^{II}_2(\mathbf{L})(dmf)_3(H_2O)_2](CF_3SO_3)_4$[a]

atom	*x*/*a*	*y*/*b*	*z*/*c*	U_{eq}	atom	*x*/*a*	*y*/*b*	*z*/*c*	U_{eq}
Cu1	0.7070(1)	0.3645(1)	0.8306(1)	0.0310(6)	C20	0.057(1)	0.277(1)	0.527(1)	0.058(7)
Cu2	0.2734(1)	0.0772(1)	0.5863(1)	0.0381(6)	C21	0.282(1)	0.2400(9)	0.6845(9)	0.029(5)
O111	0.6263(7)	0.4353(6)	0.7797(7)	0.038(4)	C22	0.324(1)	0.317(1)	0.754(1)	0.034(5)
C111	0.557(1)	0.412(1)	0.706(1)	0.048(7)	C23	0.277(1)	0.381(1)	0.754(1)	0.042(6)
N111	0.513(1)	0.4660(9)	0.673(1)	0.042(6)	C24	0.191(1)	0.367(1)	0.682(1)	0.039(6)
C112	0.428(2)	0.433(2)	0.587(2)	0.08(1)	C25	0.149(1)	0.289(1)	0.608(1)	0.037(6)
C113	0.543(2)	0.559(2)	0.716(2)	0.11(2)	C26	0.1941(9)	0.2225(9)	0.6097(9)	0.033(5)
O121	0.7317(7)	0.4231(7)	0.9741(7)	0.045(4)	C27	0.094(1)	0.092(1)	0.477(1)	0.037(6)
O211	0.3619(7)	0.0076(7)	0.6187(7)	0.040(4)	C28	0.094(1)	0.007(1)	0.430(1)	0.035(6)
C211	0.453(1)	0.033(1)	0.628(1)	0.041(6)	C29	0.017(1)	−0.050(1)	0.352(1)	0.054(7)
N211	0.5077(9)	−0.0181(9)	0.6528(9)	0.039(6)	C30	0.025(1)	−0.128(1)	0.311(1)	0.081(8)
C212	0.620(2)	0.017(2)	0.662(2)	0.05(1)	C31	0.109(1)	−0.148(1)	0.350(1)	0.067(8)
C213	0.462(2)	−0.112(1)	0.677(1)	0.060(9)	C32	0.183(1)	−0.090(1)	0.429(1)	0.048(6)
O221	0.1666(8)	−0.0340(8)	0.6532(8)	0.052(5)	S101	0.6113(3)	0.2372(3)	1.0979(3)	0.050(2)
C221	0.165(1)	−0.115(1)	0.648(1)	0.067(7)	O101	0.6262(9)	0.1667(8)	1.145(1)	0.062(6)
N221	0.146(1)	−0.172(1)	0.702(1)	0.065(7)	O102	0.7032(9)	0.3055(9)	1.094(1)	0.075(6)
C222	0.130(2)	−0.139(2)	0.781(2)	0.10(1)	O103	0.524(1)	0.204(1)	1.0184(8)	0.089(6)
C223	0.140(2)	−0.268(2)	0.682(2)	0.11(1)	C101	0.574(1)	0.306(1)	1.167(1)	0.067(8)
O231	0.3794(8)	0.1676(9)	0.5135(9)	0.051(6)	F101	0.4879(9)	0.2543(9)	1.1772(9)	0.095(7)
N1	0.8414(8)	0.4620(7)	0.8374(8)	0.035(4)	F102	0.644(1)	0.345(1)	1.2469(8)	0.134(7)
N2	0.7983(7)	0.2950(8)	0.8755(8)	0.032(4)	F103	0.559(1)	0.3769(9)	1.134(1)	0.104(7)
N3	0.5934(7)	0.2425(7)	0.8269(8)	0.033(4)	S201	0.1775(4)	0.3252(4)	0.9417(4)	0.081(2)
N4	0.4757(7)	0.1090(7)	0.8368(8)	0.032(4)	O201	0.0965(9)	0.2993(9)	0.867(1)	0.084(6)
N5	0.4084(7)	0.3073(8)	0.8122(7)	0.031(4)	O202	0.2714(8)	0.4025(7)	0.9580(8)	0.069(5)
N6	0.3383(8)	0.1838(7)	0.6964(7)	0.032(4)	O203	0.137(1)	0.337(1)	1.025(2)	0.25(1)
N7	0.1700(8)	0.1384(8)	0.5494(8)	0.034(5)	C201	0.205(2)	0.235(2)	0.976(3)	0.16(2)
N8	0.1765(8)	−0.0139(8)	0.4688(8)	0.040(5)	F201	0.128(1)	0.1572(9)	0.969(1)	0.121(9)
C1	0.860(1)	0.546(1)	0.818(1)	0.046(6)	F202	0.236(1)	0.213(1)	0.893(1)	0.18(1)
C2	0.958(1)	0.609(1)	0.828(1)	0.046(7)	F203	0.282(1)	0.251(1)	1.045(1)	0.110(8)
C3	1.038(1)	0.583(1)	0.862(1)	0.059(8)	S301	0.2023(5)	0.2442(5)	0.3304(4)	0.056(3)
C4	1.020(1)	0.495(1)	0.881(1)	0.054(8)	O301	0.105(1)	0.202(2)	0.339(1)	0.17(1)
C5	0.922(1)	0.436(1)	0.869(1)	0.038(6)	O302	0.280(2)	0.251(2)	0.403(1)	0.14(1)
C6	0.894(1)	0.341(1)	0.888(1)	0.035(7)	O303	0.217(2)	0.324(2)	0.298(2)	0.11(2)
C7	0.7461(9)	0.203(1)	0.8877(9)	0.032(5)	C301	0.195(3)	0.162(2)	0.243(3)	0.11(2)
C8	0.780(1)	0.138(1)	0.923(1)	0.039(6)	F301	0.196(2)	0.083(1)	0.275(2)	0.23(1)
C9	0.706(1)	0.0521(9)	0.931(1)	0.035(5)	F302	0.122(2)	0.137(2)	0.176(1)	0.32(2)
C10	0.602(1)	0.034(1)	0.905(1)	0.041(6)	F303	0.282(2)	0.185(1)	0.231(2)	0.19(1)
C11	0.5702(9)	0.1021(9)	0.8700(9)	0.031(5)	S401	0.6778(4)	0.2785(4)	0.5824(4)	0.082(3)
C12	0.6413(9)	0.1840(9)	0.862(1)	0.030(5)	O401	0.682(2)	0.208(2)	0.532(1)	0.18(2)
C13	0.893(1)	0.154(1)	0.953(1)	0.044(8)	O402	0.579(1)	0.285(2)	0.538(2)	0.33(2)
C14	0.741(1)	−0.024(1)	0.967(1)	0.046(7)	O403	0.707(2)	0.293(1)	0.669(1)	0.19(1)
C15	0.379(1)	0.046(1)	0.842(1)	0.044(6)	C401	0.744(5)	0.397(3)	0.559(3)	0.18(5)
C16	0.4964(9)	0.1948(9)	0.8151(9)	0.030(5)	F401	0.724(2)	0.383(2)	0.476(1)	0.20(2)
C17	0.4132(9)	0.2276(9)	0.7755(9)	0.031(5)	F402	0.829(3)	0.378(4)	0.581(3)	0.40(4)
C18	0.473(1)	0.370(1)	0.901(1)	0.043(6)	F403	0.734(2)	0.456(1)	0.593(2)	0.24(2)
C19	0.139(1)	0.435(1)	0.683(1)	0.065(8)					

[a] Esd's in terms of the least significant digit.

was collected, thoroughly rinsed with water, and dried; yield 13.57 g (94%) of an off-white powder.

Anal. Calcd for $C_{18}H_{18}N_4$: C, 74.46%; H, 6.25%; N, 19.30%. Found: C, 73.95%; H, 6.19%; N, 19.17%. ^{1}H-NMR (dmso-d_6; ppm rel to TMS): 12.98 (s, 2 NH), 7.39 (s, 4 arom H), 2.35 (s, 12 methyl H). MS: Peaks at *m*/*e* = 290 (M^+, strongest); weaker peaks at 275, 145, 137, and 130. IR (cm^{-1}): 3450 w, 3393 w, 3090 m sh, 3022 s, 2999 s, 2967 s, 2921 s, 2841 s, 2805 s, 2717 s, 2663 s, 2555 s, 2474 s, 1804 w, 1710 w, 1633 w, 1586 m, 1507 w, 1446 s, 1413 s, 1395 vs, 1328 vs, 1239 m, 1197 m, 1166 m, 1107 w, 1024 m, 1002 s, 958 vs, 864 m, 848 s, 785 w, 760 w, 730 m, 678 m, 643 w, 611 w, 571 m, 476 w, 454 w, 430 m, 329 m.

4,4′-Dinitro-5,6,5′,6′-tetramethyl-2,2′-bibenzimidazole. In a 800-mL beaker glass, 11.81 g (0.0407 mol) of 5,6,5′,6′-tetramethyl-2,2′-

Table 3. Non-Hydrogen Positional, Isotropic Displacement, and Occupation Parameters for $[Cu^{II}_4(H_2(\mathbf{L3})O_2^{2-})_2](ClO_4)_4$[a]

atom, PP	x/a	y/b	z/c	U_{eq}
Cu1	0.5	0.25	0.6080(2)	0.045(2)
Cu2	0.5	0.1729(2)	0.75	0.052(2)
O	0.532(1)	0.1863(8)	0.669(1)	0.059(8)
N1	0.535(2)	0.188(1)	0.542(1)	0.06(1)
N2	0.533(1)	0.172(1)	0.4396(9)	0.05(1)
N3	0.602(2)	0.087(1)	0.631(1)	0.05(1)
N4	0.619(2)	0.160(1)	0.762(1)	0.06(1)
C1	0.568(2)	0.111(2)	0.470(2)	0.06(1)
C2	0.593(3)	0.050(2)	0.445(2)	0.09(2)
C3	0.615(2)	0.001(2)	0.481(2)	0.06(2)
C4	0.623(2)	0.013(2)	0.541(2)	0.06(1)
C5	0.598(2)	0.073(1)	0.568(1)	0.04(1)
C6	0.563(2)	0.126(2)	0.529(2)	0.05(1)
C7	0.615(2)	0.158(1)	0.658(1)	0.04(1)
C8	0.665(2)	0.150(1)	0.711(1)	0.04(1)
C9	0.746(2)	0.140(2)	0.716(2)	0.06(1)
C10	0.784(3)	0.135(2)	0.770(2)	0.09(2)
C11	0.735(3)	0.152(2)	0.820(2)	0.07(2)
C12	0.655(2)	0.162(2)	0.819(2)	0.06(2)
C13	0.517(2)	0.215(1)	0.491(2)	0.06(1)
C14	0.528(3)	0.189(2)	0.376(2)	0.08(2)
C15, 0.5	0.463(5)	0.238(7)	0.355(3)	0.09(4)
C16	0.645(2)	−0.056(2)	0.451(2)	0.09(2)
C17	0.651(2)	−0.041(1)	0.589(2)	0.06(1)
Cl1	0.5	0.0270(6)	0.25	0.111(8)
O1, 0.5	0.5000	0.089(5)	0.2500	0.13(3)
O2, 0.5	0.531(4)	0.043(3)	0.194(3)	0.11(2)
O3, 0.5	0.415(5)	0.016(4)	0.262(5)	0.19(3)
O4, 0.5	0.447(5)	0.000(4)	0.210(4)	0.15(3)
Cl2	0.25	0.2500	0.5	0.128(8)
O5, 0.5	0.226(6)	0.204(5)	0.543(4)	0.18(3)
O6, 0.5	0.319(4)	0.225(3)	0.538(3)	0.12(2)
O7, 0.5	0.190(5)	0.271(4)	0.556(4)	0.16(3)
O8, 0.5	0.283(4)	0.316(3)	0.517(3)	0.13(2)

[a] ESD's in terms of the least significant digit.

bibenzimidazole was dissolved at room temperature in 100 mL of concentrated sulfuric acid, the resulting solution was cooled to 0 °C, and 12.5 g (0.125 mol) of 65% nitric acid was added dropwise under efficient stirring during about 10 min. The solution gradually turned intense yellow. After addition, the reaction mixture was allowed to stand at 0 °C for 10 min more; then 400 g of crushed ice was added. When the ice had melted, the yellow precipitate was filtered, washed with methanol, dried, and recrystallized from 600 mL of 2-methoxyethanol. The IR spectrum showed the resulting yellow crystals to contain 2-methoxyethanol, which was removed by drying overnight at 150 °C; yield: 11.85 g (77%) of a light yellow powder.

Anal. Calcd for $C_{18}H_{16}N_6O_4$: C, 56.84%; H, 4.24%; N, 22.09%. Found: C, 54.97%; H, 4.38%; N, 21.19%. ^{1}H-NMR (dmso-d_6, ppm rel TMS): 14.5 (s, 2 NH), 7.62 (s, 2 arom. H), 2.46 (s, 6 methyl H ortho to the nitro groups), 2.31 (s, 6 methyl H meta to the nitro groups). MS: Peaks at m/e = 380 ([M]$^+$, very strong), 363, 345, 317, 289, 110 (very strong). IR (cm^{-1}): 3509 w, 3293 vs, 2980 w, 2956 w, 2925 w, 1640 w, 1577 w, 1522 vs, 1462 m, 1443 m, 1422 m, 1386 s, 1368 s, 1321 vs, 1252 s, 1154 w, 1108 w, 1048 w, 1019 s, 989 w, 927 w, 877 m, 860 m, 797 m, 769 s, 703 w, 660 w, 638 w, 620 w, 493 w, 456 w, 401 w, 353 w.

1,1′-Dimethyl-4,4′-dinitro-5,6,5′,6′-tetramethyl-2,2′-bibenzimidazole. To 11.85 g (0.0312 mol) of 4,4′-dinitro-5,6,5′,6′-tetramethyl-2,2′-bibenzimidazole, suspended in 100 mL of dry dimethylformamide, 2.5 g (0.08 mol) of a 80% suspension of sodium hydride in mineral oil was added at room temperature. Vigorous hydrogen evolution took place and most of the product dissolved to a dark amber solution. A 10.0-g (0.070 mol) sample of methyl iodide was added at once under stirring. A yellow precipitate began to separate after a short induction period. The mixture was allowed to stand for about 3 h to complete the reaction. After addition of 5 mL of water to hydrolyze the excess sodium hydride, the precipitate was filtered, washed thoroughly with water and methanol, and dried. The yield was quantitative (12.70 g).

Anal. Calcd for $C_{20}H_{20}N_6O_4$: C, 58.82%; H, 4.94%; N, 20.58%. Found: C, 58.24%; H, 4.99; N, 20.16%. ^{1}H-NMR (dmso-d_6, ppm rel to TMS): 7.89 (s, 2 arom H), 4.23 (s, 6 *N*-methyl H), 2.48 (s, 6 methyl H ortho to the nitro groups), 2.33 (s, 6 methyl H meta to the nitro groups). MS: Peaks at m/e = 408 (M$^+$), 391, 378, 363, 348, 331, 317, 301, 287. IR (cm^{-1}): 3088 w, 3050 w, 2954 m, 2926 m, 2860 m sh, 1746 w, 1675 w, 1630 w, 1528 vs, 1480 w sh, 1460 m, 1440 s, 1407 s, 1394 s, 1379 m, 1368 s, 1338 vs, 1270 s, 1226 m, 1189 m, 1156 w, 1078 m sh, 1067 m, 1052 m sh, 1008 s, 963 m, 878 m, 822 s, 770 vs, 730 w, 662 m, 645 w, 552 w, 508 w, 468 w, 404 w, 358 w.

Table 4. Non-Hydrogen Positional, Isotropic Displacement, and Occupation Parameters for $[Cu^{I}_2(\mathbf{L3}')_2](ClO_4)_2$[a]

atom, PP	x/a	y/b	z/c	U_{eq}
Cu	0.0421(3)	0.1481(4)	0.3692(3)	0.057(4)
C1	−0.0395(17)	0.3850(27)	0.1241(22)	0.050(4)
C2	−0.0603(15)	0.4809(32)	0.1392(21)	0.050(4)
C3	−0.0738(15)	0.4937(35)	0.2044(21)	0.050(4)
C4	−0.0916(17)	0.4051(28)	0.2331(21)	0.050(4)
C5	−0.0741(15)	0.3016(29)	0.2134(19)	0.037(4)
C6	−0.0859(14)	0.2045(25)	0.2468(19)	0.037(4)
C7	−0.0985(16)	0.0158(28)	0.2318(19)	0.037(4)
C8	−0.1452(16)	−0.0444(30)	0.1889(20)	0.050(4)
C9	−0.1466(16)	−0.1480(39)	0.2127(20)	0.059(4)
C10	−0.1158(17)	−0.1941(31)	0.2764(20)	0.059(4)
C11	−0.0724(17)	−0.1242(33)	0.3136(21)	0.050(4)
C12	−0.0643(15)	−0.0236(31)	0.2984(19)	0.037(4)
C13	−0.1794(15)	−0.0002(29)	0.1199(18)	0.050(4)
C14	−0.1968(15)	−0.2186(30)	0.1620(19)	0.059(4)
C15	−0.0224(16)	−0.2436(30)	0.4182(20)	0.059(4)
C16	−0.0011(17)	−0.0522(33)	0.3953(21)	0.050(4)
C*x*	0.0387(16)	−0.2639(30)	0.4643(20)	0.059(4)
C17	0.0504(18)	−0.0277(36)	0.4559(23)	0.050(4)
C18	0.0667(17)	−0.1960(31)	0.5237(20)	0.059(4)
C19	0.2511(15)	−0.0005(32)	0.7137(19)	0.057(7)
C20	0.2484(15)	0.2134(29)	0.6459(18)	0.057(7)
C21	0.1210(19)	0.0701(34)	0.5222(23)	0.059(4)
C22	0.1273(18)	−0.0322(35)	0.5517(25)	0.059(4)
C23	0.1627(17)	−0.0621(36)	0.6216(22)	0.057(7)
O23, 0.284	0.1734(35)	−0.1595(72)	0.6578(43)	0.057(7)
C24	0.2037(17)	0.0165(33)	0.6431(20)	0.057(7)
C25	0.2087(19)	0.1188(30)	0.6152(23)	0.057(7)
C26	0.1655(18)	0.1404(39)	0.5534(22)	0.059(4)
N1	−0.0540(12)	0.2984(22)	0.1564(15)	0.037(4)
N2	−0.0874(12)	0.1196(22)	0.2066(15)	0.037(4)
N3	−0.0157(12)	0.0269(21)	0.3471(15)	0.037(4)
N4	−0.0318(12)	−0.1433(29)	0.3775(15)	0.050(4)
N5	0.0814(15)	−0.0870(28)	0.5119(19)	0.059(4)
N6	0.0737(13)	0.0652(25)	0.4614(17)	0.050(4)
N7	0.1602(12)	0.2385(25)	0.5129(15)	0.059(4)
Cl	0.1221(7)	0.5022(11)	0.5941(8)	0.083(11)
O1	0.0688(18)	0.4913(31)	0.5501(21)	0.138(15)
O2	0.1359(13)	0.6072(26)	0.6178(17)	0.103(13)
O3	0.1583(25)	0.4918(53)	0.5482(33)	0.290(36)
O4, 0.5	0.1584(24)	0.4296(45)	0.6405(30)	0.056(18)
O4′, 0.5	0.1188(28)	0.4362(50)	0.6595(33)	0.091(22)

[a] ESD's in terms of the least significant digit.

1,1′-Bridged 4,4′-Dinitro-5,6,5′,6′-tetramethyl-2,2′-bibenzimidazoles were obtained as follows: To a solution of the bibenzimidazole dianion, prepared from 3.80 g (0.01 mol) of 4,4′-dinitro-5,6,5′,6′-tetramethyl-2,2′-bibenzimidazole and 0.80 g of 80% sodium hydride suspension in 40 mL of tetramethylurea,[27] 6.00 g of the corresponding α,ω-dibromoalkane was added and the mixture was kept at 60 °C for 3 h. Thick precipitates of the respective products, mixed with sodium bromide, were obtained, and the initially deep color of the bibenzimidazole dianion was no longer perceptible. After cooling to room temperature and addition of 5 mL of water to hydrolyze excess NaH, the precipitates were filtered, washed thoroughly with water and methanol, and dried.[28]

(27) Dimethylformamide can also be used, if care is taken to avoid the presence of excessive sodium hydride, which catalyses its decomposition into dimethylamine and carbon monoxide at temperatures above 60 °C.

(28) 1,1′-Dimethylene-4,4′-dinitro-5,6,5′,6′-tetramethyl-2,2′-bibenzimidazole ($C_{20}H_{18}N_6O_4$, MW 406.40) was obtained as well as a yellow powder by reaction of the dianion with 1,2-dibromoethane, yield 4.0 g. Anal. Calcd for $C_{20}H_{18}N_6O_4$: C, 59.11%; H, 4.46%; N, 20.68%. Found: C, 59.20%; H, 5.31%; N, 18.64%. MS: M$^+$ at m/e = 406. IR similar to that of the *N,N′*-dimethyl compound.

Table 5. Selected Geometry Values (Bond Distances, Å; Bond Angles, deg) of the $[Cu_2(\mathbf{L})(dmf)_3(H_2O)_2]^{4+}$ Cation

(a) Copper Coordination Shell[a]

Cu1–N1	1.996	Cu2–N6	2.023
Cu1–N2	2.017	Cu2–N7	2.037
Cu1–N3	2.018	Cu2–N8	2.021
Cu1–O111	1.942	Cu2–O211	1.952
Cu1–O121	2.284	Cu2–O231	2.392
Cu1–O403	2.742	Cu2–O221	2.471
N1–Cu1–N2	81.0	N6–Cu2–N7	83.2
N2–Cu1–N3	83.4	N7–Cu2–N8	80.3
N3–Cu1–O111	100.4	N8–Cu2–O211	96.2
O111–Cu1–N1	94.8	O211–Cu2–N6	100.2
sum in plane	359.6	sum in plane	359.9
N1–Cu1–N3	164.0	N6–Cu2–N8	163.4
N2–Cu1–O111	174.5	N7–Cu2–O211	174.9
N1–Cu1–O121	93.0	N6–Cu2–O231	92.7
N2–Cu1–O121	88.9	N7–Cu2–O231	92.7
N3–Cu1–O121	90.7	N8–Cu2–O231	90.1
O111–Cu1–O121	95.0	O211–Cu2–O231	90.9
N1–Cu1–O403	81.7	N6–Cu2–O221	92.9
N2–Cu1–O403	83.2	N7–Cu2–O221	92.4
N3–Cu1–O403	92.5	N8–Cu2–O221	85.8
O111–Cu1–O403	92.6	O211–Cu2–O221	83.7

(b) Ligand (Averaged over the 2-Fold Pseudosymmetry)[b]

N1–C1	1.318(4)	C7–C8	1.385(16)
C1–C2	1.381(2)	C8–C9	1.426(12)
C2–C3	1.363(5)	C9–C10	1.382(2)
C3–C4	1.374(4)	C10–C11	1.383(3)
C4–C5	1.274(8)	C11–C12	1.372(2)
C5–N1	1.358(3)	C12–C7	1.399(6)
C5–C6	1.455(1)	C13–C8	1.517(2)
C6–N2	1.279(3)	C14–C9	1.519(14)
N2–C7	1.411(5)		
C11–N4	1.387(3)	C15–N4	1.463(5)
N4–C16	1.347(4)		
C16–N3	1.322(14)	C16–C17	1.486(–)
N3–C12	1.390(2)		
N1–C5–C6	115.1(4)	N3–C16–N4	113.7(11)
C5–C6–N2	116.9(1)	C16–N4–C11	106.6(11)
C6–N2–C7	131.4(3)	N4–C11–C12	105.2(7)
N2–C7–C12	109.8(8)	C11–C12–N3	111.0(5)
C7–C12–N3	125.6(7)	C13–C8–C9	120.7(7)
C12–N3–C16	103.6(1)	C14–C9–C8	119.9(4)
N3–C16–C17	123.4(2)	C15–N4–C16	127.5(5)

[a] O111 and O211 are the two equatorial dmf oxygen atoms, O121 and O231 are the two axial water oxygen atoms, O221 is the axial dmf oxygen, and O403 is the axial trifluoromthanesulfonate oxygen atom. The metal–metal distance, Cu1···Cu2, is 6.160 Å, and the dihedral angle between the coordination subunits is $\tau = 117.3°$. The two coordinated water molecules form hydrogen bridges to the trifluoromethanesulfonate anions: O121···O102, 2.81 Å; O121···O202(1), 2.81 Å ((1) = $(1 - x, 1 - y, 2 - z)$); O231···O302, 2.68 Å; O231···O402, 2.77 Å. Trifluoromethanesulfonate 4 binds directly to Cu1 via O403 and indirectly to Cu2 via the hydrogen bridge O402···O231. The dihedral angle between the two coordination subunits may depend on this feature. [b] Standard deviations of the average in parentheses.

1,1′-Trimethylene-4,4′-dinitro-5,6,5′,6′-tetramethyl-2,2′-bibenzimidazole. The reaction with 1,3-dibromopropane afforded 4.2 g (100%) of a bright yellow powder. Anal. Calcd for $C_{21}H_{20}N_6O_4$: C, 59.99%; H, 4.79%; N, 19.99%. Found: C, 58.11%; H, 5.15%; N, 18.51%. MS: $[M]^+$ at $m/e = 420$.

1,1′-Tetramethylene-4,4′-dinitro-5,6,5′,6′-tetramethyl-2,2′-bibenzimidazole. The reaction with 1,4-dibromobutane afforded 4.3 g (100%) of a faint yellow powder. Anal. Calcd for $C_{22}H_{22}N_6O_4$: C, 60.82%; H, 5.10%; N, 19.34%. Found: C, 57.78%; H, 5.24%; N, 18.83%. MS: $[M]^+$ at $m/e = 434$.

1,1′-Dimethyl-4,4′-diamino-5,6,5′,6′-tetramethyl-2,2′-bibenzimidazole. In a 500-mL beaker glass, 8.11 g (0.02 mol) of 1,1′-dimethyl-4,4′-dinitro- 5,6,5′,6′-tetramethyl-2,2′-bibenzimidazole were dissolved in 100 mL of concentrated hydrochloric acid, and 50.0 g (0.22 mol) of hydrated tin dichloride was added in portions to the yellow solution. A precipitate formed initially, followed by a slow exothermic reaction. Heating to 100 °C led to complete dissolution, and after 15 min an almost colorless solution resulted. After 1 h of reflux, the mixture was cooled and diluted with 150 mL of water to precipitate the chlorostannate of the protonated amine, which was isolated on a sintered glass filter funnel and treated twice with 20 mL of a 20% NaOH solution in order to liberate the amine and to remove the tin(IV) as the soluble sodium hydroxostannnate. The remaining precipitate was washed thoroughly with water and dried to yield 5.57 g (81%) of product.

Anal. Calcd for $C_{20}H_{24}N_6$: C, 68.94%; H, 6.94%; N, 24.12%. Found: C, 67.44%; H, 7.09%; N, 22.30%. ^{1}H-NMR (dmso-d_6, ppm rel to TMS): 6.69 (s, 2 arom H), 5.02 (s, 4 NH), 4.17 (s, 6 *N*-methyl H), 2.36 (s, 6 methyl H meta to the amino groups) and 2.13 (s, 6 methyl H ortho to the amino groups). MS: Peaks at $m/e = 348$ ($[M]^+$, strong), 333, 174. IR (cm^{-1}): 3468 m, 3444 m, 3370 s, 3195 w, 2962 m sh, 2928 m, 2908 m, 2856 m, 2726 w, 1621 vs, 1492 s, 1462 m, 1439 s, 1412 m, 1381 m, 1360 m, 1340 vs, 1282 m, 1253 m, 1152 w, 1100 m, 1070 m, 1020 w, 1000 m, 805 s, 682 m, 665 m, 631 w, 581 m, 470 w, 353 w.

Following the procedure described for the 1,1′-dimethyl derivative, we obtained as well the following:

Table 6. Selected Geometry Values (Bond Distances, Å; Bond Angles, deg) for the $[Cu_4(H_2(\mathbf{L3})O_2^{2-})_2]^{4+}$ Cation

Copper Coordination Spheres

Cu1–O	1.92(2)	Cu2–O	1.89(3)
Cu1–N1	1.99(3)	Cu2–N4	1.96(3)
N1–Cu1–O	92.5(8)	N4–Cu2–O	83.1(9)
N1–Cu1–N1′	85.(1)	N4–Cu2–N4″	165.2(9)
O–Cu1–O′	90.2(8)	O–Cu2–O″	163.8(7)
N1–Cu1–O′	176.6(9)	N4–Cu2–O″	99.0(9)
sum in plane	360.2	sum in plane	364.2

Cu_4O_4 Unit

Cu1···Cu1‴	6.297(7)	O···O′	2.722(5)
Cu1···Cu2	3.498(4)	O···O″	3.737(5)
Cu2···Cu2′	3.048(6)	O···O‴	4.386(5)
Cu2···Cu1···Cu2′		51.7(1)	
Cu1···Cu2···Cu1‴		128.3(2)	
Cu1–O–Cu2	134.(1)	O′–Cu1–O–Cu2	25.0
O–Cu1–O′	90.2(8)	Cu1–O–Cu2–O″	–38.8
O–Cu2–O″	163.8(7)		

Ligand

C5–N3	1.41(4)	C7–C8	1.44(4)
N3–C7	1.54(3)	C7–O	1.47(3)
C5–N3–C7		124.(2)	
N3–C7–O	107.(2)	Cu1–O–Cu2	134.(1)
O–C7–C8	115.(2)	Cu2–O–C7	111.(2)
C8–C7–N3	107.(2)	C7–O–Cu1	112.(2)
sum at C7	329	sum at O	357
C6–C5–N3–C7	–31.9	C5–N3–C7–C8	–144.2
C5–N3–C7–O	92.4	N3–C7–C8–N4	–107.9
N1–C13–C13′–N1′	–7.4		

Table 7. Selected Geometry Values (Bond Distances, Å; Bond Angles, deg) for the $[Cu_2(\mathbf{L3}')_2]^{2+}$ Cation

Copper Coordination Sphere

Cu–N1′	2.00(3)	N1′–Cu–N2′	81.(1)
Cu–N2′	2.11(3)	N3–Cu–N6	82.(1)
Cu–N3	2.00(3)	N1′–Cu–N3	143.(1)
Cu–N6	2.01(3)	N1′–Cu–N6	132.(1)
		N2′–Cu–N3	99.(1)
		N2′–Cu–N6	115.(1)
C12–C7–N2–Cu′	103	N6–C17–C16–N3	5
Cu···Cu′	4.59(2)		

dihedral angle at the copper ion: $\omega = 79.1°$

Scheme 1. Synthesis of the 2,2′-bibenzimidazole Based Cavitands

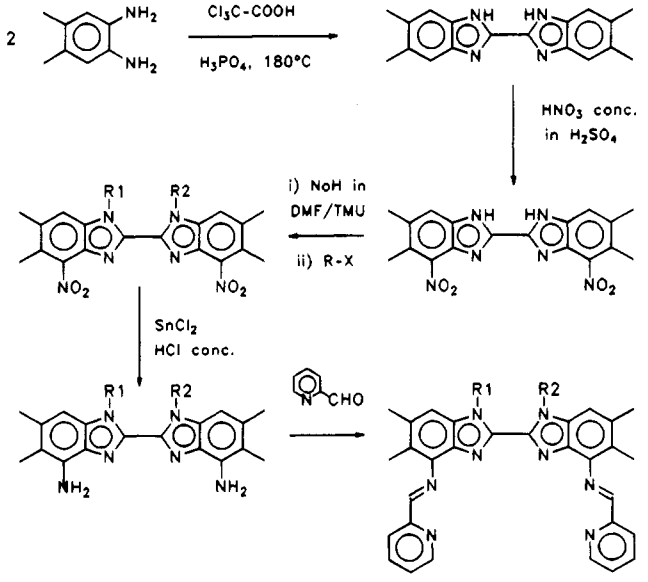

1,1′-Trimethylene-4,4′-diamino-5,6,5′,6′-tetramethyl-2,2′-bibenzimidazole. Anal. Calcd for $C_{21}H_{24}N_6$: C, 69.97%; H, 6.71%; N, 23.31%. Found: C, 62.07%; H, 6.66%; N, 19.73%. MS: $[M]^+$ at m/e = 360 (the product was contaminated with about 20% of an unidentified species with m/e = 394).

1,1′-Tetramethylene-4,4′-diamino-5,6,5′,6′-tetramethyl-2,2′-bibenzimidazole. Anal. Calcd for $C_{22}H_{26}N_6$: C, 70.56%; H, 7.00%; N, 22.44%. Found: C, 63.34%; H, 7.20%; N, 18.94%. MS: $[M]^+$ at m/e = 374 (this product too was contaminated with about 10% of an unidentified species with m/e = 408).

These two compounds were used without further purification in the subsequent Schiff base condensation reaction, the crystallization of the Schiff base representing the necessary purification step.

1,1′,5,5′,6,6′-Hexamethyl-4,4′-bis(2-picolinimino)-2,2′-bibenzimidazole (L). A 3.48-g sample of 1,1′-dimethyl-4,4′-diamino-5,6,5′,6′-tetramethyl-2,2′-bibenzimidazole was dissolved in 60 mL of boiling dimethylformamide, containing a drop of acetic acid. A 3.00-g sample of 2-pyridinecarboxaldehyde, dissolved in 15 mL of 2-methoxyethanol, was added at once under stirring, and a yellow color gradually developed. The mixture was heated briefly to reflux and allowed to cool, when a voluminous crystallization occurred. After 2 h, the crystals were filtered, washed with methanol, and dried to yield 4.45 g (85%) of light yellow flakes.

Anal. Calcd for $C_{32}H_{30}N_8$: C, 72.98%; H, 5.74%; N, 21.28%. Found: C, 71.94%; H, 5.71%; N, 21.07%. ^{1}H-NMR ($CDCl_3$, ppm rel to TMS; py = pyridine, bz = benzimidazole): 9.54 (s, 2 imine H), 8.75 ("d", 2 py H), 8.44 ("d", 2 py H), 7.85 ("t", 2 py H), 7.39 ("t", 2 py H), 7.12 (s, 2 arom bz H), 4.30 (s, 6 *N*-methyl H), 2.52 (s, 6 methyl H), 2.51 (s, 6 methyl H). MS: $[M]^+$ strongest peak at m/e = 526; decay peaks at 511, 448, 437, 422, 407, 359, 348, 333 and 318. IR (cm^{-1}): 3050 w, 3000 w, 2935 w sh, 2905 m, 2890 w sh, 2860 w sh, 1710 w, 1680 w, 1615 m, 1585 s, 1565 s, 1470 s, 1450 w, 1435 s, 1425 w sh, 1405 s, 1395 s, 1380 m, 1360 w sh, 1320 s, 1290 m, 1275 m, 1240 w, 1220 s, 1145 w, 1120 vw, 1080 s, 1065 m sh, 1040 m, 1005 m, 995 s, 965 s, 950 m, 875 w, 860 w, 815 s, 780 m, 760 s, 735 s, 715 w, 665 s, 650 w sh, 620 m, 585 w, 575 m, 490 s, 475 m, 435 w, 405 m, 365 w sh, 350 m, 335 w.

1,1′-Trimethylene-5,5′,6,6′-tetramethyl-4,4′-bis-(2-picolinimino)-2,2′- bibenzimidazole (L3). Anal. Calcd for $C_{33}H_{30}N_8$: C, 73.58%; H, 5.61%; N, 20.80%. Found: C, 71.53%; H: 5.53%; N, 20.15%. MS: $[M]^+$ at m/e = 538; decay peaks at 460, 434, 360, 348, 345, and 207.

1,1′-Tetramethylene-5,5′,6,6′-tetramethyl-4,4′-bis(2-picolinimino)-2,2′- bibenzimidazole (L4). Anal. Calcd for $C_{34}H_{32}N_8$: C, 73.89%; H, 5.84%; N, 20.27%. Found: C, 71.52%; H, 6.02%; N, 19.99%. MS: $[M]^+$ at m/e = 552; decay peaks at 474, 448, 374, 359, and 207.

$[Cu^{II}_2(L)(dmf)_3(H_2O)_2](CF_3SO_3)_4$. A 0.45-g sample of the Schiff base ligand **L** (0.85 mmol) and 0.61 g of $Cu(CF_3SO_3)_2$ (1.70 mmol) were dissolved in 10 mL of dmf to yield an olive-green solution. Wet diethyl ether (50 mL) was added to form a two-layer system, and the flask was stoppered. Upon standing for 3 days, green prisms had crystallized from the dark green lower layer. These crystals were isolated, washed with dmf/ether (1:5), and dried to yield 1.155 g (90%) of crystals suitable for X-ray work.

Anal. Calcd for $C_{45}H_{55}Cu_2F_{12}N_{11}O_{17}S_4$: C, 35.91%; H, 3.68%; N, 10.24%. Found: C, 35.86%; H, 3.63%; N, 10.28%. IR (cm^{-1}): 3440 s, 3400 m sh, 3260 w, 3100 w sh, 3070 w, 3040 w, 2950 w sh, 2920 w, 2860 vw, 1655 vs, 1605 m, 1490 m, 1475 m, 1450 m sh, 1440 m, 1410 m, 1390 m, 1370 m, 1350 m, 1280 vs, 1250 vs, 1225 vs, 1160 vs, 1105 m, 1030 vs, 920 w, 880 w, 860 w, 845 w, 790 w sh, 780 w, 770 w, 760 w, 740 w, 720 w, 700 w, 690 w sh, 660 m sh, 640 s, 570 m, 555 w, 510 m, 495 w, 480 w sh, 420 w, 385 w.

Oxygenation of Cu(I) Complexes. A 0.270-g sample of **L3** was added to a solution of 0.328 g of $[Cu(MeCN)_4]ClO_4$ in 20 mL of analytical grade acetonitrile. A deep brown solution (of $[Cu^I_2(\mathbf{L3})](ClO_4)_2$) immediately formed, which was allowed to stand under air in a capped flask. After a week, a crystalline deposit had formed, and a microscopic investigation revealed the presence of two different types of crystals, a dichroic green/red orthorhombic compound and a brown monoclinic one. This experience was repeated several times, until a crop of sufficiently well developed crystals was obtained, which could be characterized by X-ray analysis.[29]

The oxygenation experiment was also carried out with **L** and with **L4** in place of **L3**, yielding a totally different result. When 0.260 g of **L** was added to a solution of 0.328 g of $[Cu(MeCN)_4]ClO_4$ in 20 mL of acetonitrile under admission of air, a green precipitate of a copper(II) compound immediately deposited. This compound was insoluble in common organic solvents, indicating the presence of a coordination polymer. When 0.140 g of **L4** was added to a solution of 0.160 g $[Cu(MeCN)_4]ClO_4$ in 20 mL of acetonitrile under air, a red-brown solution of the copper(I) complex formed first, as in the case of **L3**, which eventually turned to a dark green copper(II) compound within a few seconds. No crystalline product was deposited in this case. Similarly, the addition of 0.270 g of **L3** to a solution of 0.361 g of copper(II) triflate in 15 mL of acetonitrile resulted in a brown-green solution of the corresponding copper(II) complex without any deposition of crystals.

Results and Discussion

$[Cu^{II}_2(L)(dmf)_3(H_2O)_2](CF_3SO_3)_4$.[30] The structure of the cation (Figures 1 and 6) (Figure 6 is given in the supplementary material) confirms the correct identity of the ligand **L**, as well as its ability to coordinate two metal ions. The structural results are consistent with the EPR and UV/vis data; both copper ions are present in a normal elongated octahedral coordination environment with the characteristic (4 + 2) geometry, too far from each other (Cu−Cu = 6.16 Å) to give rise to a detectable magnetic interaction. The dihedral angle between the two coordination subunits of 115.7° reflects a compromise between the high electrostatic repulsion of the two Cu^{2+} ions which would be present in the *cis*-coplanar conformation of the ligand and the high steric interaction between the copper coordination

(29) Direct structural characterization is in such cases a superior tool to any other analytical method, since it allows one to look at the products closest to the primary reaction. Copper complexes are labile, and a recrystallization step is likely to change composition and structure of certain compounds. These X-ray determinations had to be carried out on relatively small crystals, i.e., at the lower limit of the sensitivity range. However, a knowledge of the strongest 15% of the structure factor amplitudes is already sufficient to establish composition and structure of a compound unambiguously and without any prior knowledge, although the molecular geometry in such a case may not be very accurate.

(30) Three of the four trifluormethanesulfonate anions (S201, S301, S401) showed high anisotropic temperature factors as well as a poor geometry, as a consequence of partial rotational disorder. Refinement of these groups as a disordered 2-position isotropic model resulted, however, in a considerably higher *R*-value, so that the original model was retained finally. The highest peak in the final difference fourier map was 0.33 e* A^{-3}, close to the disordered sulfur atom S401.

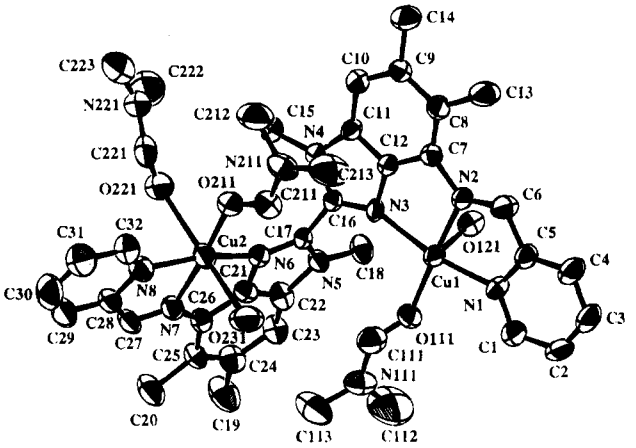

Figure 1. Atom labeling scheme of the $[Cu^{II}_2(\mathbf{L})(dmf)_3(H_2O)_2]^{4+}$ cation. O(121) and O231 are the two water oxygen atoms. The triflate anions have label numbers 101−103, 201−203, 301−303, and 401−403.

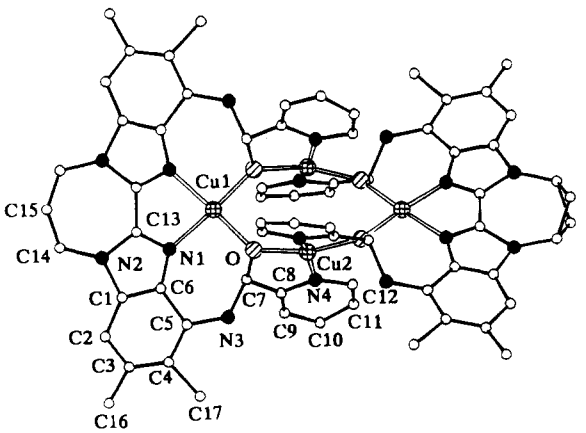

Figure 2. Atom labeling scheme of the $[Cu^{II}_4(H_2(\mathbf{L3})O_2^{2-})_2]^{4+}$ cation. The perchlorate anions are labeled (Cl1, O1···O4) and (Cl2, O5···O8).

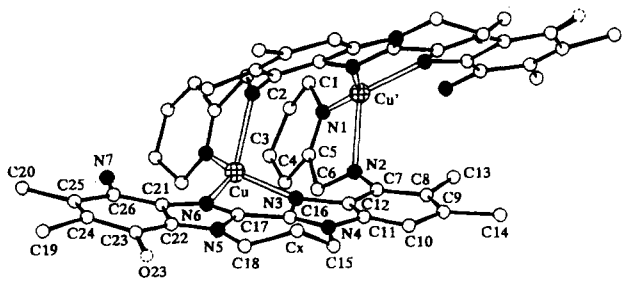

Figure 3. Atom labeling scheme of the $[Cu^{I}_2(\mathbf{L3'})_2]^{2+}$ cation. The perchlorate anion is labeled (Cl, O1···O4). The oxygen atom O23 (indicated as a dashed circle) corresponds to the oxidized fraction of L3′.

shells and the *N*-methyl groups in the corresponding *trans*-coplanar conformation. The presence of an electrostatic interaction between the two copper ions is also evident from the cyclic voltammogram, which shows two distinct Cu(II)/Cu(I) reduction waves, separated by 0.30 V (*vide infra*). The situation is thus similar to the complexes described by Karlin,[31] which prefer an open conformation, except in the presence of a negatively charged and strongly coordinating bridging ligand like imidazolate or azide, able to assemble the positively charged ions together.

The coordination environments of the two copper(II) ions consist of each three equatorial nitrogen atoms of the ligand **L** (⟨Cu−N⟩ = 2.02 Å), the fourth ligand in the plane being a

(31) Cf. ref 8h.

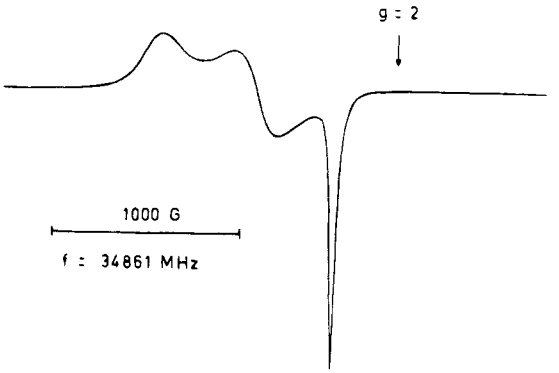

Figure 4. Q-band (34′861 MHz) EPR spectrum of $[Cu^{II}_2(\mathbf{L})(dmf)_3(H_2O)_2](F_3CSO_3)_4$ in the solid state (rhombic: $g_1 = 2.225$, $g_2 = 2.129$, $g_3 = 2.067$).

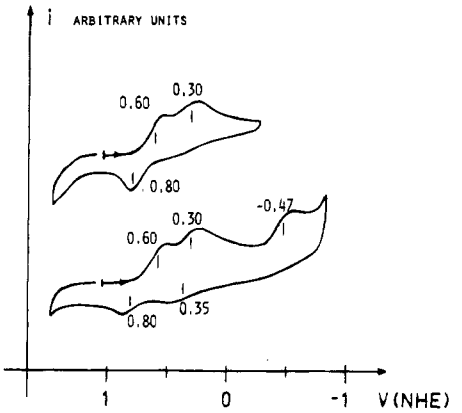

Figure 5. Cyclic voltammogram of $[Cu^{II}_2(\mathbf{L})(dmf)_3(H_2O)_2](F_3CSO_3)_4$ in acetonitrile (0.1 M TBAP) at a glassy carbon electrode.

dimethylformamide (dmf) oxygen atom (⟨Cu−O⟩ = 1.95 Å). The sum of the equatorial X−Cu−X angles is very close to 360° at both copper ions, indicating a planar arrangement. The axial ligands are further away from the copper centers but still within generally accepted coordination distances: two water oxygen atoms at 2.28 and at 2.39 Å respectively of Cu1 and Cu2, a dmf oxygen atom at 2.47 Å of Cu1, and a trifluormethanesulfonate (triflate) oxygen atom at 2.74 Å of Cu(2). The two copper ions are thus inequivalent. The coordinating triflate makes a hydrogen bond to the axial water molecule of the neighboring copper ion; this may be determinant of the actually observed dihedral angle between the two coordination subunits of the ligand.

The organic part of the molecule shows largely the expected bond lengths and angles.[32] The angles N1−C5−C6 (115.1°), C5−C6−N2 (116.9°), and N2−C7−C12 (109.8°) are, however, significantly smaller than the expected 120° of an unconstrained sp^2 type atom; a consequence of the coordination to a metal ion, which "draws together" the ligand framework. Further details of the geometry are given in Table 5. The crystal packing (supplementary material, Figure 10) consists of alternating layers of complex cations and trifluormethanesulfonate anions.

The effect of an internal rotation around the ligand's central single bond (C16−C17 of the bibenzimidazole moiety) onto the Cu···Cu distance was studied with the help of computed molecular models, based on the present structural data of $[Cu^{II}_2(\mathbf{L})(dmf)_3(H_2O)_2](CF_3SO_3)_4$: It follows that the two copper ions can approach each other down to a minimal distance of 3.15 Å in the *cis*-coplanar conformation of the ligand. A

(32) Allen, F. H.; Kennard, O.; Watson, D. G.; Brammer, L.; Orpen, A. G.; Taylor, R. *J. Chem. Soc., Perkin Trans. 2* **1987**, S1−S19.

rotation of 27° out of the *cis*-coplanar conformation would result in a hemocyanin like copper−copper distance of 3.55 Å. The ligand could be constrained to such a conformation by the introduction of a trimethylene bridge into its bibenzimidazole backbone, in the place of the two methyl groups. This insight triggered the synthesis and investigation of the ligand **L3**.

EPR Spectrum. The Q-band EPR powder spectrum of $[Cu^{II}_2(\mathbf{L})(dmf)_3(H_2O)_2](CF_3SO_3)_4$ (Figure 4), taken at 34 861 MHz and 23 K, is strongly rhombically distorted with $g_1 = 2.225$, $g_2 = 2.129$, and $g_3 = 2.067$. The lines corresponding to g_1 and g_2 are considerably broader than the g_3 line, a fact which is attributable to the expected, but not resolved, copper (^{63}Cu, ^{65}Cu) and nitrogen (^{14}N) fine structure, as well as to the presence of two slightly different copper environments. Such a big rhombic splitting is, however, not *a priori* expected for a monomeric N_3O copper site. Karlin et al. reported a high rhombic splitting and broad lines in the case of a *p*-xylyl bridged N_3Cl_2 dicopper(II) complex (with a Cu···Cu distance of 11.7 Å), where the corresponding monomeric analogues showed a quite normal, tetragonal spectrum.[33] Claims to some kind of interaction between the copper ions in our system are thus founded, although we did not observe any half field signal in the spectrum.

UV/Vis Spectra. A solution of the complex in propylenecarbonate showed a single broad ligand field absorption with maximum at 665 nm, typical of a square planar Cu(II) chromophore. Below 450 nm, ligand to metal charge transfer and ligand centered absorptions were present, explaining the green color of the complex.

Electrochemistry. The cyclic voltammogram of $[Cu^{II}_2(\mathbf{L})(dmf)_3(H_2O)_2](CF_3SO_3)_4$ (Figure 5) shows two distinct, "irreversible" Cu(II)/Cu(I) reduction waves at 0.60 and 0.30 V (NHE), followed by a further wave at −0.47 V (probably a Cu(I)/Cu(0) reduction). The reoxidations to Cu(II) take place at 0.35 and 0.80 V (NHE); the relatively big potential difference of 200 mV between the first reduction and the last oxidation wave indicates that considerable geometric changes are taking place in the coordination spheres of the copper ions following the electron transfer reaction. For comparison, a natural type 3 site shows a value of 0.36 V (NHE).[4]

Oxygenation Reactions of Cu(I) Compounds. The dicopper(I) complex of the trimethylene bridged ligand **L3** gave rise to a peculiar behavior, compared to its congeners **L** and **L4**, when submitted to the oxygenation reaction. Whereas an immediate oxidation to the green copper(II) compound was observed in the case of **L**, the solutions of $[Cu^{I}_2(\mathbf{L3})](ClO_4)_2$ in acetonitrile were quite stable in closed flasks in the presence of air, and only after standing for days at room temperature, a crystalline deposit was obtained, which turned out to be a mixture of an orthorhombic Cu(II) compound, $[Cu^{II}_4(H_2(\mathbf{L3})O_2^{2-})_2](ClO_4)_4$, and a monoclinic copper(I) compound, $[Cu^{I}_2(\mathbf{L3'})_2](ClO_4)_2$. The former represents an oxidation product of the primaryly formed $[Cu^{I}_2(\mathbf{L3})](ClO_4)_2$, whereas the latter may be thought to be a degradation product of the Cu(II) complex, with half of the pyridine−carboxaldehyde functionalities missing (*vide infra*). In the case of the more flexible, tetramethylene bridged ligand **L4**, a brown solution of the copper(I) complex was formed upon mixing, just as with **L3**. Under air, it turned to a green copper(II) compound, however, already within a few seconds. The flexible **L4** seems to adopt an intermediate position between the completely free **L** and the restricted **L3**.

Structure of $[Cu^{II}_4(H_2(\mathbf{L3})O_2^{2-})_2](ClO_4)_4$.[34] This cation, $[Cu^{II}_4(H_2(\mathbf{L3})O_2^{2-})_2]^{4+}$, (Figures 2 and 7), is a tetranuclear copper cluster with a symmetric, eight membered Cu_4O_4 core consisting of four Cu^{2+}, bridged by four oxygen atoms. The whole is held together by two **L3** ligands, which are covalently linked to the O-atoms of the Cu_4O_4 core via the azomethine carbon atoms (forming the **L3** derivative $H_2(\mathbf{L3})O_2^{2-}$). The former azomethine nitrogen atoms carry each a proton and do no longer coordinate. The pyridyl group of the ligand make a dihedral angle of 58° with the bibenzimidazole unit. The two **L3** units are furthermore inclined by 43° with respect to each other, giving the cation a particular aspect in longitudinal projection (supplementary material, Figure 8).

Both copper ions are in square planar coordination environments; no axial ligands are present, but there are two different copper(II) coordination modes: a *cis*-CuN_2O_2 and a *trans*-CuN_2O_2 one. *cis*-CuN_2O_2 is made up by Cu1, the 2,2′-bibenzimidazole group, and the bridging oxygen atoms and is completely planar, as seen from the sum of the in-plane angles of 360°. *trans*-CuN_2O_2 consists of Cu2, the pendant pyridyl groups, and the bridging oxygen atoms; it has a slight saddle shape, as indicated by the sum of the in-plane angles of 364°. The bridging oxygen atom is trigonal planar within the standard deviation. Further details of the geometry are given in Table 6. The crystal packing (supplementary material, Figure 11) shows a three-dimensional network of interstacked cations with the disordered perchlorate anions occupying the voids. There is an indication of weak hydrogen bonding between the protonated former azomethine nitrogen atoms and the perchlorate anions. The formation of this compound can be explained by an autoxidation reaction in the presence of water:

$$2[Cu^{I}_2(\mathbf{L3})](ClO_4)_2 + 2H_2O + O_2 \rightarrow [Cu^{II}_4(H_2(\mathbf{L3})O_2^{2-})_2](ClO_4)_4$$

Structure of $[Cu^{I}_2(\mathbf{L3'})_2](ClO_4)_2$.[35] The cation, $[Cu^{I}_2(\mathbf{L3'})_2]^{2+}$ (Figures 3 and 9), is a dimeric (dinuclear) copper(I) cluster, where **L3′** is a degradation product of the original ligand **L3**. The coordination environment of the two symmetry related copper(I) ions is a distorted N_4-tetrahedron, made up of each a 2,2′-bibenzimidazole unit of **L3′** and a picolinimine unit of its symmetry equivalent. The Cu−N bond lengths (⟨2.04 Å⟩) as well as the chelate bite angles (⟨82°⟩) are in the expected range.[36] The dihedral angle between the two chelating diimine units at the copper ion is 79°, and the Cu···Cu distance is 4.59 Å. The picolinimine part of the ligand is rotated out of the bibenzimidazole plane by 70° and coordinates to the other copper ion of the dimer. The two bibenzimidazole units of the dimer make an angle of 40° toward each other, giving the cation the aspect of a semiopened shell. The crystal packing (supplementary material, Figure 12) consists of a regular, three-dimensional array of complex cations and perchlorate anions without any particular features.

The ligand **L3′** derives from the original **L3** through cleavage (hydrolysis) of one of the two pending picolinimines, regenerating a free aromatic amino group on one side of the bibenzimi-

(33) Karlin, K. D.; Hayes, J. C.; Zubieta, J. In *Copper Coordination Chemistry: Biochemical and Inorganic Perspectives*; Karlin, K. D., Zubieta, J., Eds.; Adenine: New York, 1983; pp 457−472, and references cited therein. See also ref 8i.

(34) Only a relatively small crystal was available, with the consequence of rather high standard deviation of the measured data. The two ClO_4^- are in special positions (2-fold axis and inversion center, respectively) and show considerable disorder. This explains the high final *R*-value.

(35) Only a small crystal was available. Nevertheless, the structure could be solved and refined without problems, using constraints on the displacement parameters of the atoms. Only the copper and chlorine atoms were refined anisotropically. The perchlorate anion is disordered. The standard deviations of the atom positions are rather high, due to the low fraction of observed data.

(36) Cf. Müller, E.; Piguet, C.; Bernardinelli, G.; Williams, A. F. *Inorg. Chem.* **1988**, *28*, 849.

Scheme 2. Degradation Products of Ligand **L3** (with Acronyms)

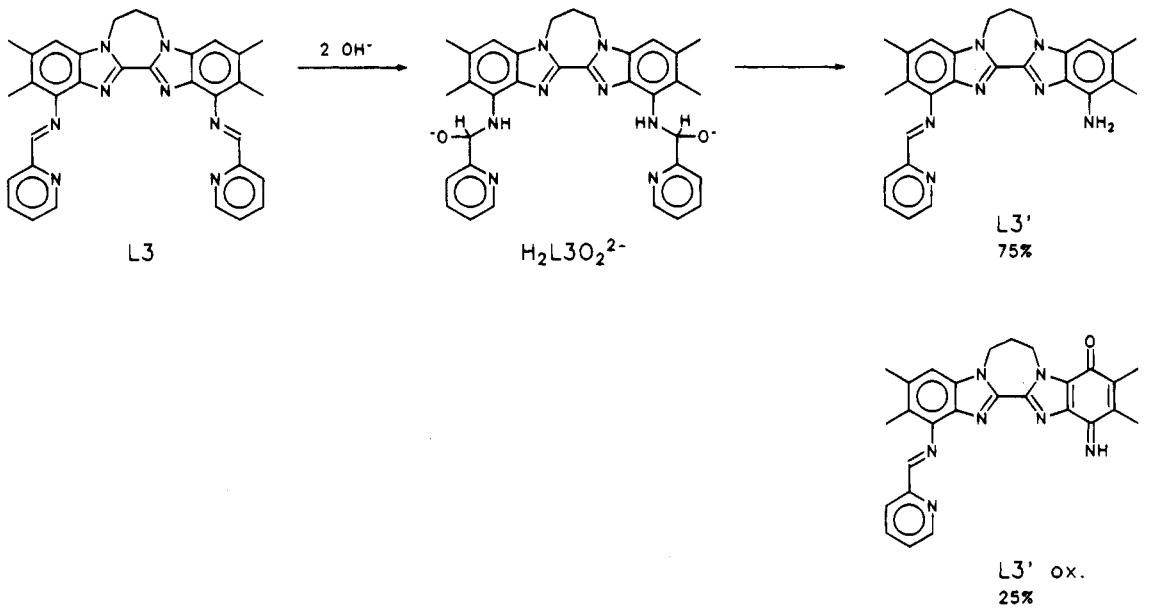

dazole backbone. During the refinement of the X-ray structure, a relatively strong residual peak was found at a distance of 1.2 Å from the carbon C2), *para* to the free amino group. It was thus apparent that the benzene ring carrying the free amino group was partially oxidized to the corresponding *p*-quinoneimine (Scheme 2). An oxygen atom O23, introduced at this position, refined to a population coefficient of 0.28(4). This means that about a quarter of the available amine sites are oxidized. The experimental findings are explained if this second cation is a degradation product of $[Cu^{II}_4(H_2(\mathbf{L3})O_2^{2-})_2]^{4+}$, formed according to

$$[Cu^{II}_4(H_2(\mathbf{L3})O_2^{2-})_2]^{4+} \rightarrow [Cu^{I}_2(\mathbf{L3'})_2]^{2+} + 2Cu^{2+} + 2C_5H_4N{-}CHO + 2(OH^-)$$

The oxidation of a quarter of the two ligand's aromatic amine sites to quinoneimines would correspond to the reduction of the two internal copper ions from the +II to the +I state. Such a reaction is facilitated by the pseudotetrahedral N_4-environment of the copper centers, which confers them a relatively high redox potential.

Conclusions

Our versatile ligand system allows us to bring together two metal ions rigidly at a given distance, providing at the same time for a void between them. In this respect it reproduces in part the situation in natural hemocyanin. Other ligand systems, which were proposed so far as coordination chemical hemocyanin models, needed either a directly coordinating structural element, like a phenolate or an alkoxy group, in order to bridge the copper ions together, or, in its case, it was the peroxo group itself which assembled the two halves of the model and acted as a bridge.

The here presented 2,2'-bibenzimidazole based ligand class is a promising step on the way to organic molecules which preestablish all the structural requirements for an optimal metal–dioxygen binding, imitating an important part of the protein's function in the natural type 3 site. The assembling and protecting role of the protein is still a widely neglected aspect of bioinorganic modeling, and our results on the particular behavior of ligand **L3** in the oxygenation of copper(I) are already proof of its importance. Although we did not yet manage to isolate the corresponding dicopper–μ-peroxo (oxy-) species with the present ligands, the results are strongly encouraging the synthesis of the originally aimed and sterically more protected systems proposed in Chart 2, in the hope of obtaining finally a room temperature stable oxy-species which mimics the situation in natural hemocyanins.

Acknowledgment. We are indebted to Mr. S. Gorter and Dr. R. A. G. de Graaff (Leiden Institute of Chemistry (LIC) for collecting the data of two X-ray structures and help in their solution. We thank further Dr. J. G. Haasnoot, Mr. G. A. van Albada, and Mr. R. A. M. van der Hoeven (LIC) for many useful discussions and for assistance with the analyses of ligands and complexes. Dr. S. P. J. Albracht, University of Amsterdam, is acknowleged for recording the Q-band EPR spectrum. Dr. P. Péchy, EPFL Lausanne, is acknowledged for measuring the NMR spectra. E.M. thanks the "Schweizerischer Nationalfonds zur Förderung der wissenschaftlichen Forschung" for a grant for advanced researchers, permitting him to perform this work.

Supporting Information Available: For the three structures, $[Cu^{II}_2(\mathbf{L})(dmf)_3(H_2O)_2](CF_3SO_3)_4$, $[Cu^{II}_4(H_2(\mathbf{L3})O_2^{2-})_2](ClO_4)_4$ and $[Cu^{I}_2(\mathbf{L3'})_2](ClO_4)_2$, respectively, tables anisotropic displacement parameters (Tables 8–10), calculated positions of hydrogen atoms (Tables 11–13), and molecular least squares planes and their intersection angles (Tables 14–16) and figures showing stereo and profile drawings of the cations (Figures 6–9) and crystal packing diagrams (Figures 10–12) (13 pages). Ordering information is given on any current masthead page.

IC950262F